Journal of Power Sources 257 (2014) 156–162

Contents lists available at ScienceDirect

Journal of Power Sources

journal homepage: www.elsevier.com/locate/jpowsour

Au- and Pd-modified porous Co film supported on Ni foam substrate as the high performance catalysts for H_2O_2 electroreduction

Fan Yang, Kui Cheng, Ke Ye, Xue Xiao, Fen Guo, Guiling Wang, Dianxue Cao*

Key Laboratory of Superlight Material and Surface Technology of Ministry of Education, College of Material Science and Chemical Engineering, Harbin Engineering University, Harbin 150001, China

HIGHLIGHTS

- Electrodeposition of Co film for spontaneous deposition of Au or Pd is reported.
- The 3D porous electrode exhibits good catalytic performance for H_2O_2 reduction.
- The 3D porous electrode is consisted of numerous interconnected nanoparticles.

ARTICLE INFO

Article history:
Received 18 August 2013
Received in revised form
20 January 2014
Accepted 21 January 2014
Available online 31 January 2014

Keywords:
Gold
Palladium
Cobalt film
Spontaneous deposition
Surface-modification
Hydrogen peroxide electroreduction

ABSTRACT

Non-noble metal film electrode (Co/Ni foam) modified with noble metals (Au and Pd) has been reported. Highly porous Co film is firstly prepared electrochemically on the commercial Ni foam substrate and in turn serves as a hard template and a redox inducer for modification by spontaneous deposition of Au or Pd. The electrodes (Au-modified Co/Ni foam and Pd-modified Co/Ni foam) are characterized by scanning electron microscopy equipped with energy dispersive X-ray spectrometer, and X-ray diffractometer. The catalytic performance of the 3D porous electrodes is evaluated by voltammetry and chronoamperometry. Results reveal that Au- and Pd-modified Co/Ni foam exhibit excellent catalytic performance and good stability for H_2O_2 electroreduction compared with Au and Pd particles supported on Ni foam, benefitting from the unique 3D structure which can ensure high utilization of catalyst and quick releases of gas bubbles produced by H_2O_2 decomposition from the electrode.

1. Introduction

Fuel cells are a promising power-generation technology for the direct conversion of chemical energy into electricity. They play a crucial role in solving the problems of energy crisis and environmental pollution. In recent years, H_2O_2-based fuel cells, such as direct methanol–hydrogen peroxide fuel cell [1–3], direct borohydride–hydrogen peroxide fuel cell [4–6], hydrazine–hydrogen peroxide fuel cell [7–9] and direct peroxide–peroxide fuel cell [10–15], have been widely investigated. Note that H_2O_2 is often used as oxidant instead of O_2 in these types of liquid-based fuel cells, indicating that improving H_2O_2 electroreduction performance could further improve the cell performance. Generally, given remarkable physicochemical properties of noble metals in the Pt group, they are considered as the best catalysts for electrochemical reaction [16–19]. However, recent studies [20] have reported that Pt-based catalysts alone account for 38–56% of the cost of polymer electrolyte membrane fuel cells, and the cathode consumes around 90% of Pt catalysts because of its sluggish oxygen reduction reaction (ORR) kinetics. Being a more economic and plentiful metal than Pt, Au has been investigated for its electrocatalytic activity [21–24], furthermore, it has also been demonstrated to have no significant catalysis to H_2O_2 decomposition unlike Pt and other noble metals, ensuring the high utilization efficiency of H_2O_2 [25]. Pd has also attracted considerable attention because it has very similar properties to Pt (e.g., same group of the periodic table, same *fcc* crystal structure, and similar atomic size) while being less expensive and more abundant than Pt [26,27]. Indeed, Au and Pd have been studied intensively as the most promising Pt-free catalysts.

In order to further reduce the cost of catalysts and improve the cell performance, many researchers have focused on the preparation of nanostructures with various special morphology and size. Currently, nanoporous foam materials represent a very promising type of structured materials having a number of interesting, even

* Corresponding author. Tel./fax: +86 451 82589036.
E-mail address: caodianxue@hrbeu.edu.cn (D. Cao).

0378-7753/$ – see front matter © 2014 Elsevier B.V. All rights reserved.
http://dx.doi.org/10.1016/j.jpowsour.2014.01.100

unique properties and through this method, many non-noble/noble metal and -based foams can be successfully prepared [28–30]. Kiani and co-workers [30] have present indirect fabrication of Ag and Pd foams based on electrochemical deposition of scarified Cu foam at a Cu sheet, and spontaneous galvanic replacement. The groups of Yu and Huang [31] have prepared porous Pd and PdNi using hydrogen bubble dynamic template and they have also proved that the catalysts exhibit excellent catalytic activity and stability towards methanol oxidation. Fabricated foam electrodes show electrocatalytic properties with several benefits. First, the procedure is very simple and fast and can perform at room temperature using commercially available reagents in water as a green solvent with no need to any additive. Second, based on this method, we could design catalysts and metal foams for practical application since it is possible to save the usage of precious metals like Au, Pd and Ag, only by surface modification of other cheap metals. In fact, the catalyst on the surface is the actual catalytic active species, implying that the inner catalyst has little catalysis. Interestingly, the coated amount of noble metals on the surface of metal foam could be also easily controlled. Their great potential for rapid electrochemical reactions arising from the high surface area and superior mass transport, makes Au- and Pd-modified Co/Ni foam electrodes the potential candidates for the application in fuel cells.

In the present paper, we described the preparation of Au and Pd-modified porous Co film electrodes via a two-step procedure: at first, the electrodeposition of porous Co film on Ni foam substrate at high current density, then the spontaneous deposition of Au and Pd by immersion of the Co deposits in the solutions containing Au and Pd ions (Eqs. (1) and (2)).

$$Co(0) + Pd^{2+} \rightarrow Co^{2+} + Pd(0) \quad (1)$$

$$3Co(0) + 2Au^{3+} \rightarrow 3Co^{2+} + 2Au(0) \quad (2)$$

We report a study aiming to significantly improve the utilization of precious Au and Pd catalysts and their catalytic performance. We chose Ni foam as the substrate due to its high electrical conductivity and a desirable open 3D structure. A 3D porous Co particle layer was electrodeposited on Ni foam which greatly increases the surface area of Ni foam substrate. The obtained 3D Au and Pd-modified Co/Ni foam electrode exhibit high catalytic performance and good stability for electroreduction of H_2O_2.

2. Experimental

2.1. Preparation and characterization of Au and Pd-modified Co/Ni foam electrodes

The Au and Pd-modified Co/Ni foam electrodes were prepared in two steps. Step one consisted of electrodeposition of porous Co film by applying a constant current of -2.0 A cm^{-2} for 100 s to electrochemical cell, containing 0.1 mol L^{-1} $CoSO_4$ + 1.0 mol L^{-1} $(NH_4)_2SO_4$ + 0.7 mol L^{-1} NH_4OH aqueous solution. The growth of Co film was accompanied by gas evolution at all times until the electrochemical deposition was terminated. The spontaneous deposition of Au was performed by immersion of the porous Co layers in the solution containing 1.0 mmol L^{-1} $HAuCl_4$ + 0.1 mol L^{-1} NaCl for 30 s. The same procedure was followed for Pd-modified Co/Ni foam electrode in 1.0 mmol L^{-1} Na_2PdCl_4 + 0.1 mol L^{-1} NaCl for 10 s. Prior to use, the Ni foam (10 mm × 10 mm × 1.1 mm, 110 PPI, 320 g m^{-2}; Changsha Lyrun Material Co., Ltd. China) was degreased with acetone, etched with 6.0 mol L^{-1} HCl for 5 min, and then rinsed with deionized water extensively. For comparative study, Ni foam supported Au particles (Au/Ni foam) and Pd particles (Pd/Ni foam) were also prepared by the same method as that for Au- and Pd-modified Co/Ni foam without porous Co film deposits. The depositions were carried out in a three-electrode electrochemical cell controlled by computerized potentiostat (Autolab PGSTAT302, Eco Chemie). The Ni foam served as the working electrode, which was placed between two pieces of platinum foil in parallel as the counter electrodes. A saturated calomel electrode (SCE) was used as the reference electrode.

The electrode morphology was characterized by a scanning electron microscope (SEM, JEOL JSM-6480) equipped with an energy dispersive X-ray spectrometer (EDX). The structure was analyzed using an X-ray diffractometer (Rigaku TTR III) with Cu K radiation (λ = 0.1514178 nm). The Au and Pd loading were measured using an inductive coupled plasma emission spectrometer (ICP, Xseries II, Thermo Scientific). Au and Pd in the 1.0 cm^2 electrodes was first dissolved in aqua regia solution and then diluted to 1 L solution for the ICP measurement.

2.2. Electrochemical measurements

The catalytic performance of the Au and Pd-modified Co/Ni foam electrodes for H_2O_2 electroreduction was measured by linear scan voltammetry and chronoamperometry with the same configuration as that for electrodeposition with the exception that the two Pt foil counter electrodes were placed behind D-porosity glass frits. The electrolyte for H_2O_2 electroreduction was H_2O_2-containing KOH solution. The reported current densities were calculated using the geometrical area of the electrode. All solutions were made with analytical grade chemical reagents and ultra-pure water (Milli-Q 18 MΩ cm). All measurements were performed at ambient temperature (20 ± 2 °C) under N_2 atmosphere.

3. Results and discussion

3.1. Characterization of porous Co film and Au-modified Co/Ni foam electrode

Fig. 1 shows the low and high-magnification SEM images of porous Co film supported on commercial Ni foam substrate, fabricated by electrodeposition in an electrolyte of 0.1 mol L^{-1} $CoSO_4$ + 1.0 mol L^{-1} $(NH_4)_2SO_4$ + 0.7 mol L^{-1} NH_4OH at a constant cathodic current of -2 A cm^{-2} for 100 s. It can be observed from Fig. 1A that the as-prepared Co film was uniformly covered on the surface of Ni foam skeleton and exhibited a 3D porous structure with highly porous nanoramified walls, with diameters of some micrometres (Fig. 1B), left by hydrogen bubbles that evolve at large cathodic current density (-2 A cm^{-2}). Much narrower pores were also visible. More importantly, the walls of the Co film consisted of numerous interconnected nanoparticles and showed continuous nanopores. Additionally, the surface of the 3D porous Co film exhibited a wrinkle appearance, consisting of an assembly of flake-like structures with rippled morphology due to its ultrathin feature. Evidently, the numerous nanoflakes with a lateral size of several hundred nanometers were intercrossed with each other, creating loose porous nanostructures with abundant open space and electroactive surface sites (Fig. 1C and D), providing a superior framework for Au or Pd modification.

In order to prepare the Au-modified Co/Ni foam electrode, the as-fabricated Co film electrode was then rapidly transferred to a solution containing 1.0 mmol L^{-1} $HAuCl_4$ + 0.1 mol L^{-1} NaCl for 30 s. As seen from Fig. 2A, the initial morphology of porous Co deposits was still well-preserved after the spontaneous deposition of Au. Fig. 2B and C shows that Au is uniformly distributed on the surface of Co nanoparticles and the surface of the as-formed Co film becomes rougher. The Au surfaces can be fully utilized because all the Au particles are accessible to H_2O_2 and electrolytes. Besides,

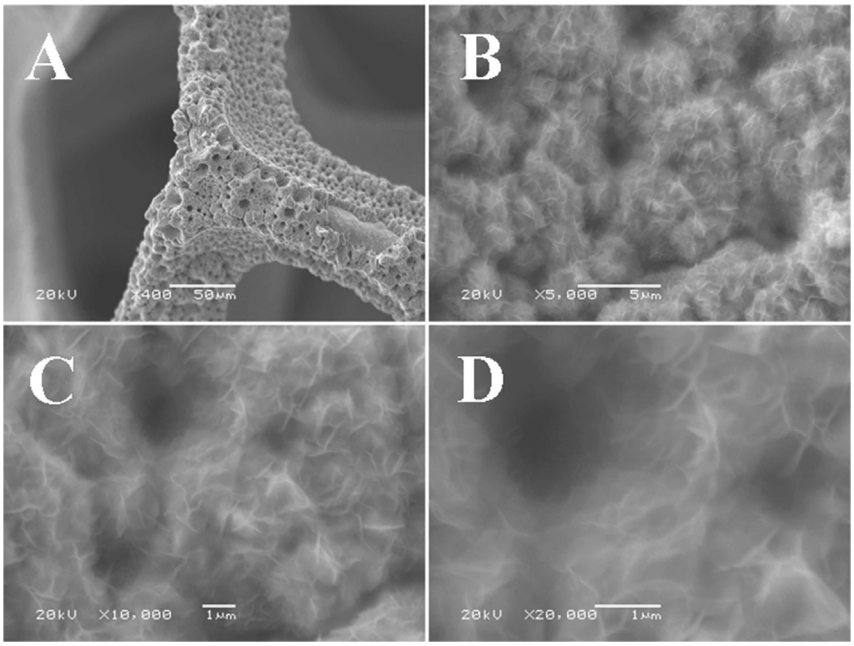

Fig. 1. Low and high-magnification SEM images of porous Co film, fabricated by electrodeposition in an electrolyte of 0.1 mol L^{-1} $CoSO_4$ + 1.0 mol L^{-1} $(NH_4)_2SO_4$ + 0.7 mol L^{-1} NH_4OH at a constant cathodic current of −2 A cm^{-2} for 100 s.

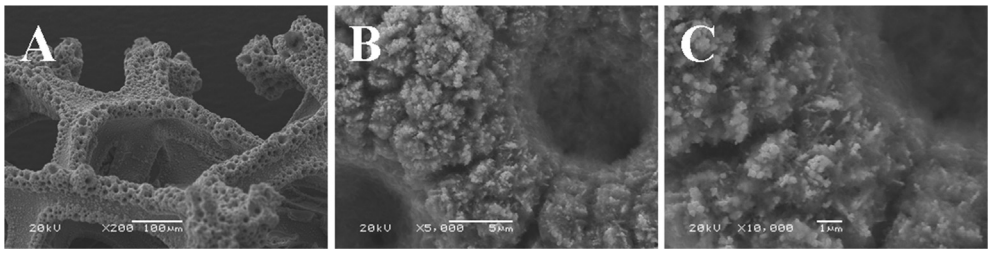

Fig. 2. Low and high-magnification SEM images of Au-modified Co/Ni foam electrode, prepared by immersing the Co film in an aqueous solution containing 1.0 mmol L^{-1} $HAuCl_4$ + 0.1 mol L^{-1} NaCl for 30 s.

oxygen gas generated by H_2O_2 hydrolysis can quickly diffuse away from the electrode, preventing surface active sites of Au from blocking by adsorbed gas bubbles.

Fig. 3A–D show the SEM image and the mapping of Au, Co and Ni elements obtained by EDX analysis. As seen, the distribution of Au is crater-like having the same outline with the morphology of Au-modified Co/Ni foam electrode, suggesting that Au is uniformly distributed on the surface of Co. Energy dispersive X-ray (EDX) spectroscopy was used to characterize the surface composition of the obtained Au-modified Co/Ni foam electrode (Fig. 3E). The spectrogram of the EDX measurement shows that two characteristic peaks of the metallic Au peaks are observed at 9.712 and

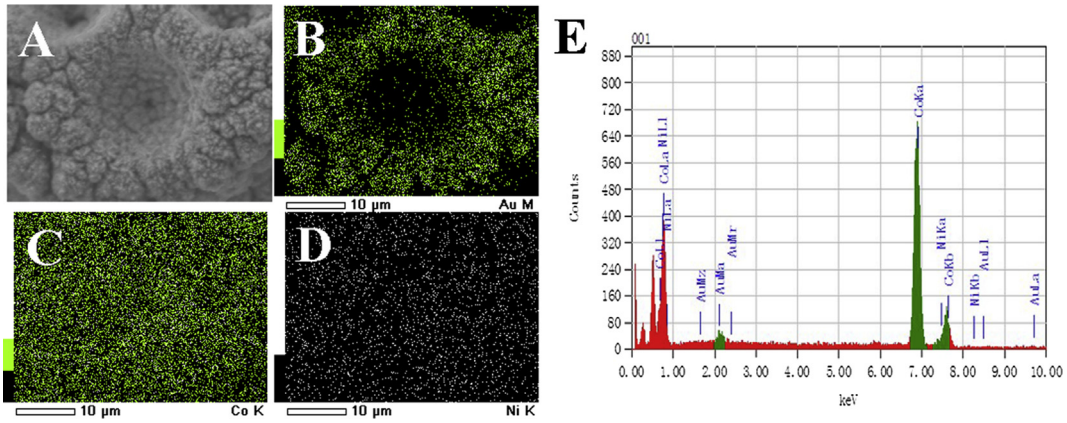

Fig. 3. The SEM image (A), the corresponding elemental distributions of Au, Co and Ni (B–D) and the corresponding EDX spectrum (E) of Au-modified Co/Ni foam electrode.

2.122 keV, which are in agreement with Au La and Ma, respectively [32], and the content of Au was clearly lower than Co, which can be also demonstrated from the data obtained by ICP measurements (0.2415 mg cm^{-2}).

To further determine the structure and composition of the as-prepared samples, XRD patterns of Ni foam substrate, porous Co film and Au-modified Co/Ni foam electrode are also shown in Fig. 4. There exist three sharp diffraction peaks at 44.5°, 51.8° and 76.3° in each XRD pattern, which can be indexed to the diffraction from the (111), (20 0) and (220) planes of Ni metal according to the standard crystallographic spectrum of Ni (JCPDS card No. 65-2865), originating from the Ni foam substrate. Moreover, the diffraction intensities of Ni foam are dramatically diminished after electrodeposition of Co film, suggesting that the porous Co film is uniformly covered upon the Ni foam surface. After replacement with Au by spontaneous deposition, a new peak at 38.2° was observed, which can be ascribed to the (111) plane of Au (JCPDS card No. 65-2870) (The inset of Fig. 4). Due to the low loading, the diffraction intensity of Au is much weaker.

3.2. Electrocatalytic activity of Au-modified Co/Ni foam electrode for H_2O_2 electroreduction

The electrocatalytic activity for H_2O_2 electroreduction was investigated using Au-modified Co/Ni foam electrode as a model system. Fig. 5A shows the cyclic voltammograms (CV) of Ni foam substrate, porous Co film and Au-modified Co/Ni foam electrode in KOH solution. The CV profile of the Ni foam substrate only shows a strong oxidation peak (centered at 0.29 V) and a reduction peak (centered at 0.18 V), which is due to the redox reactions of Ni^{2+}/Ni^{3+} according to the literature [10,28]. The porous Co film displays the typical features of Co metal, which is in consistence with that reported previously [33] and the redox peaks can be attributed to the inter-conversion of Co to $Co(OH)_2$ to $Co(OH)_3$. After Au deposition, it can be observed that, the two pairs of redox peaks of Co became larger which may cause from the hydrogen adsorption/desorption and the redox reaction of Au on the Au-modified Co/Ni foam electrode, similar to those reported in the literature for Au electrode in alkaline solution [34,35].

In order to further demonstrate that the Au-modified Co/Ni foam electrode is the superior electrocatalyst for H_2O_2 reduction, we also systematically evaluate the electrochemical performance by means of cyclic voltammetry and chronoamperometry. The cost of catalysts is a major problem for the development of fuel cells, so how to improve the efficiency of catalyst is a hotspot. To directly explain the efficiency of Au on the Au-modified Co/Ni foam electrode, the current density unit was expressed as A cm^{-2} mg^{-1}. Fig. 5B shows the influence of KOH concentration for H_2O_2 reduction, with the fixed H_2O_2 concentration at 0.5 mol L^{-1} and the changing KOH concentration from 1.0 mol L^{-1} to 4.0 mol L^{-1}. As seen, too high KOH concentration could not lead to the high performance. Inset of Fig. 5B is the comparative cyclic voltammograms of Au-modified Co/Ni foam electrode, porous Co film and Au/Ni foam in 3.0 mol L^{-1} KOH containing 0.5 mol L^{-1} H_2O_2. The Au-modified Co/Ni foam electrode displays much higher H_2O_2 electroreduction currents than porous Co film and Pd//Ni foam electrode in the potential range of −0.2 V to −0.5 V. At −0.3 V, a reduction current density on Au-modified Co/Ni foam electrode can reach to −0.66 A cm^{-2} mg^{-1}, and that obtained on Au/Ni foam electrode is only −0.16 A cm^{-2} mg^{-1}. A limiting current density of 1.08 A cm^{-2}m g^{-1} is obtained at the negative sweep, which is also much larger than that on Au particles supported on Ni foam [6], demonstrating the superior electrocatalytic activity of Au-modified Co/Ni foam electrode.

The effects of H_2O_2 concentration were also investigated in Fig. 5C. When the concentration of H_2O_2 is lower than 0.5 mol L^{-1}, the H_2O_2 electroreduction reached to diffusion control at −0.42 V, and the reduction current density remarkably increased with the increase of H_2O_2 concentration from 0.25 mol L^{-1} to 1.5 mol L^{-1}. We noticed that the decomposition of H_2O_2 becomes apparent at high concentration of H_2O_2. So low H_2O_2 concentration should be used in practice to avoid the influence of chemistry decomposition of H_2O_2 on the electrochemical measurements. In summary, the suitable ratio of [KOH]/[H_2O_2] was found to be 3:1.

The stability of Au-modified Co/Ni foam electrode for H_2O_2 electroreduction was investigated by chronoamperometric measurements. Fig. 5D shows chronoamperometric curves of H_2O_2 electroreduction on the Au-modified Co/Ni foam electrode. The potentials were selected in the region from the open circuit potential to peak potential according to the CVs (Fig. 5B and C). At −0.25 V, current densities reached steady-state after a few seconds and displayed no decrease within 30 min test period, indicating that the Au-modified Co/Ni foam electrode has a good stability for catalyzing H_2O_2 electroreduction. At higher potential (−0.3 V and −0.35 V), current densities slightly decreased, which may result from the depletion of H_2O_2 near the electrode surface. The same electrode was used in the whole measurement at the three potentials, that is, the electrode was actually examined for 5400 s.

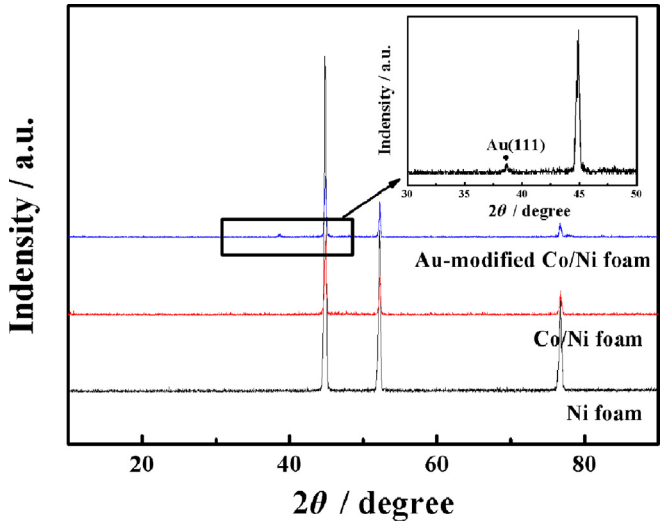

Fig. 4. XRD patterns of Ni foam substrate, porous Co film supported on Ni foam and Au-modified Co/Ni foam electrode. Inset is the zoom of the diffraction peak of Au.

3.3. Characterization of Pd-modified Co/Ni foam electrode

The main goal of this study aims at fabrication of noble metal surface-modification of other cheaper metals to improve the efficiency of noble metals. In brief, the applicability of proposed method for fabrication of Pd-modified Co/Ni foam electrode was also evaluated. Fig. 6 shows the different magnification SEM images of Pd-modified Co/Ni foam electrode, prepared by immersing the Co film in an aqueous solution containing 1.0 mmol L^{-1} Na_2PdCl_4 + 0.1 mol L^{-1} NaCl for 10 s. Similar to the results in Fig. 2, the introduction of Pd cannot damage the highly porous structure of the as-prepared Co film, and uniformly covered on the surface of Co deposits.

EDX spectrum analysis of Pd-modified Co/Ni foam electrode was also taken and the results were shown in Fig. 7. The mapping of Pd element obtained by EDX analysis has the same outline with the

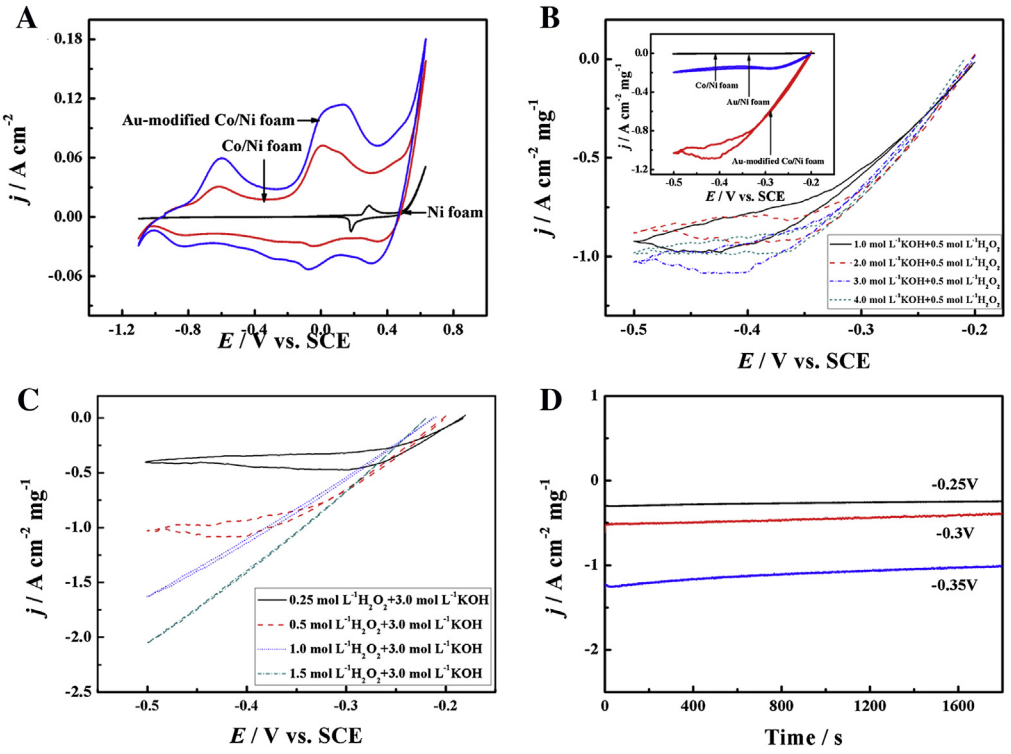

Fig. 5. Cyclic voltammograms of Ni foam, porous Co film and Au-modified Co/Ni foam electrode in 1.0 mol L^{-1} KOH at a scan rate of 50 mV s^{-1} (A); The effects of KOH concentration for H_2O_2 electroreduction (B); The effects of H_2O_2 concentration for H_2O_2 electroreduction (C); Chronoamperometric curves for H_2O_2 electroreduction at different potentials in 3.0 mol L^{-1} KOH + 1.0 mol L^{-1} H_2O_2 (D). The inset of B is the zoom of the comparative cyclic voltammograms of porous Co film, Au/Ni foam and Au-modified Co/Ni foam electrodes in 3.0 mol L^{-1} KOH + 0.5 mol L^{-1} H_2O_2.

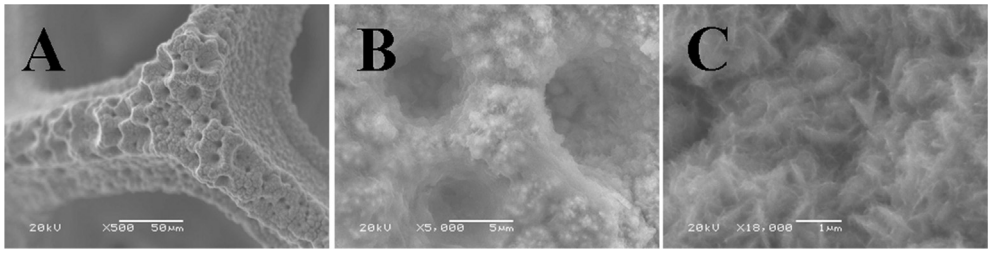

Fig. 6. Low and high-magnification SEM images of Pd-modified Co/Ni foam electrode, prepared by immersing the Co film in an aqueous solution containing 1.0 mmol L^{-1} Na_2PdCl_4 + 0.1 mol L^{-1} NaCl for 10 s.

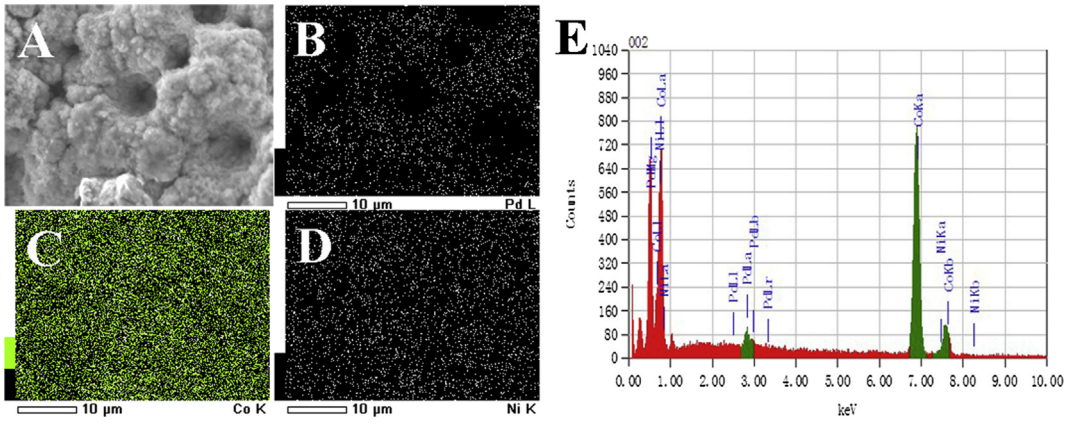

Fig. 7. The SEM image (A), the corresponding elemental distributions of Pd, Co and Ni (B–D) and the corresponding EDX spectrum (E) of Pd-modified Co/Ni foam electrode.

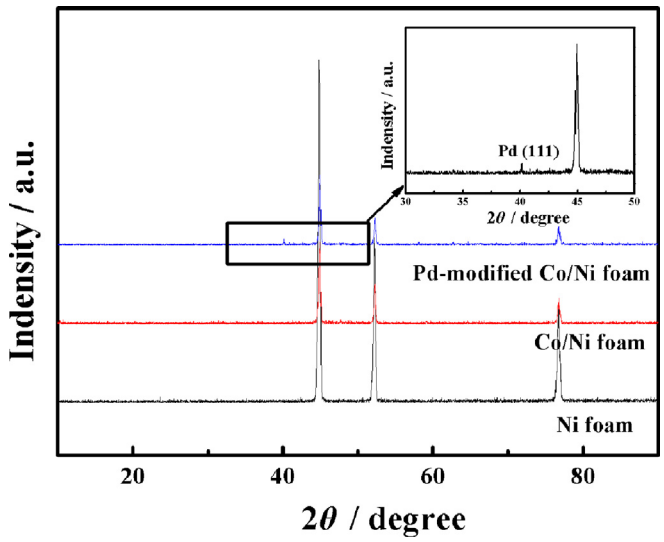

Fig. 8. XRD patterns of Ni foam substrate, porous Co film supported on Ni foam and Pd-modified Co/Ni foam electrode. Inset is the zoom of the diffraction peak of Pd.

surface of Pd-modified Co/Ni foam electrode in the corresponding SEM image (Fig. 7A), suggesting that Pd displayed a well-uniform distribution on the surface of porous Co film. Apparently, the content of Pd was much lower than Co, resulting from the low content of Pd (0.1291 mg cm^{-2}). The mapping of Ni element came from the Ni foam substrate. The spectrogram of the EDX measurement also exhibited the characteristic peaks of the metallic Pd according to previous literature [30].

XRD measurements of Ni foam substrate, porous Co film supported on Ni foam and Pd-modified Co/Ni foam electrode were also carried out. The partial enlarged view of XRD pattern of Pd-modified Co/Ni foam electrode was presented in the inset of Fig. 8 to clearly reveal the diffraction peak of Pd. Due to the low loading of Pd on the Pd-modified Co/Ni foam electrode, the typical diffraction peak of Pd (111) plane at 40.1° according to the standard crystallographic spectrum of Pd (JCPDS card No. 65-2867), was also much weaker.

3.4. Electrocatalytic activity of Pd-modified Co/Ni foam electrode for H_2O_2 electroreduction

The catalytic performance and stability of Pd-modified Co/Ni foam electrode towards H_2O_2 electroreduction was also systematically examined in this work and the results were displayed in Fig. 9. Obviously, a reduction peak (center at ~−0.56 V) can be observed on the CV curve of Pd-modified Co/Ni foam electrode resulting from the reduction of PdO formed on the surface of electrode, which exhibits the typical features of polycrystalline Pd in alkaline solution reported in the previous literature [12]. Besides, the redox pairs of Co also become larger due to the enhancement of the hydrogen adsorption/desorption on Pd and the redox reaction between Pd and PdO. We also tested the influence of KOH and H_2O_2 concentration of H_2O_2 electroreduction on the as-prepared Pd-modified Co/Ni foam electrode. The comparative polarization curves for H_2O_2 electroreduction on porous Co film, Pd/Ni foam and Pd-modified Co/Ni foam electrodes were also displayed in Fig. 9. At −0.3 V, a reduction current density on Pd-modified Co/Ni foam electrode can reach to −0.96 A cm^{-2} mg^{-1}, and that obtained on Pd/Ni foam electrode is only −0.31 A cm^{-2} mg^{-1}. A peak reduction current density of 1.85 A cm^{-2} mg^{-1} is obtained in the solution of

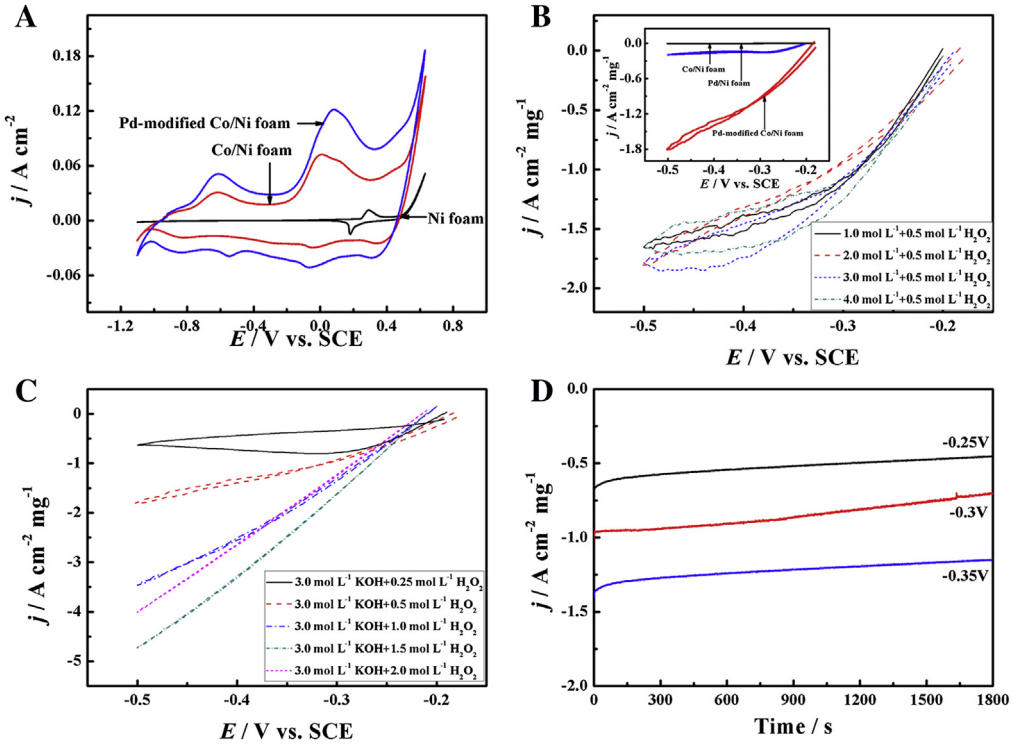

Fig. 9. Cyclic voltammograms of Ni foam, porous Co film and Pd-modified Co/Ni foam electrode in 1.0 mol L^{-1} KOH at a scan rate of 50 mV s^{-1} (A); The effects of KOH concentration for H_2O_2 electroreduction (B); The effects of H_2O_2 concentration for H_2O_2 electroreduction (C); Chronoamperometric curves for H_2O_2 electroreduction at different potentials in 3.0 mol L^{-1} KOH + 1.0 mol L^{-1} H_2O_2 (D). The inset of B is the zoom of the comparative cyclic voltammograms of porous Co film, Pd/Ni foam and Pd-modified Co/Ni foam electrodes in 3.0 mol L^{-1} KOH + 0.5 mol L^{-1} H_2O_2.

3.0 mol L^{-1} KOH + 0.5 mol L^{-1} H_2O_2. In summary, the electrode possesses excellent catalytic activity and good stability for H_2O_2 electroreduction from Fig. 9B–D.

4. Conclusion

A simple and green approach for fabricating noble metals (Au and Pd) surface-modification of non-noble metal (Co) was developed. The electrochemically fabricated porous Co film supported on Ni foam substrate was used as a scarifying hard framework for modification by spontaneous deposition of Au or Pd. In order to exhibit the superior electrocatalytic performance, we have further examined the catalytic performance and stability of Au- and Pd-modified Co/Ni foam electrodes towards H_2O_2 electroreduction. The 3D porous electrodes, consisting of interconnected microparticles, exhibited excellent catalytic performance and good stability for H_2O_2 electroreduction. The limiting reduction current densities of 1.08 A cm^{-2} g^{-1} and 1.85 A cm^{-2} g^{-1} are obtained at the Au- and Pd-modified Co/Ni foam electrodes, respectively. The enhanced performance is ascribed to the unique structure of electrode, which ensures high utilization of catalysts and quick releases of gas bubbles produced by H_2O_2 decomposition from the electrodes. The novel porous electrode has a great potential for the application in fuel cells due to its facile preparation, high performance and low cost.

Acknowledgments

We gratefully acknowledge the Fundamental Research Funds for the Central Universities (HEUCF20130910013) and National Nature Science Foundation of China (21306033).

References

[1] J. Zhu, R.R. Sattler, A. Garsuch, O. Yepez, P.G. Pickup, Electrochim. Acta 51 (2006) 4052–4060.
[2] L. Li, Y. Zhang, J. Power Sources 175 (2008) 256–260.
[3] J.R.C. Salgado, J.C.S. Fernandes, A.M. Botelho do Rego, A.M. Ferraria, R.G. Duarte, M.G.S. Ferreira, Electrochim. Acta 56 (2011) 8509–8518.
[4] C. Celik, F.G. Boyaci San, H.I. Sarac, Int. J. Hydrogen Energy 35 (2010) 8678–8682.
[5] C. Celik, F.G. Boyaci San, H.I. Sarac, Fuel Cells 12 (2012) 1027–1031.
[6] D. Cao, Y. Gao, G. Wang, R. Miao, Y. Liu, Int. J. Hydrogen Energy 35 (2010) 807–813.
[7] A. Serov, C. Kwak, Appl. Catal. B Environ. 98 (2010) 1–9.
[8] W.X. Yin, Z.P. Li, J.K. Zhu, H.Y. Qin, J. Power Sources 182 (2008) 520–523.
[9] T. Sakamoto, K. Asazawa, U. Martinez, B. Halevi, T. Suzuki, S. Arai, D. Matsumura, Y. Nishihata, P. Atanassov, H. Tanaka, J. Power Sources 234 (2013) 252–259.
[10] A.E. Sanli, A. Aytaç, Int. J. Hydrogen Energy 36 (2011) 869–875.
[11] F. Yang, K. Cheng, X. Liu, S. Chang, J. Yin, C. Du, L. Du, G. Wang, D. Cao, J. Power Sources 217 (2012) 569–573.
[12] F. Yang, K. Cheng, Y. Mo, L. Yu, J. Yin, G. Wang, D. Cao, J. Power Sources 217 (2012) 562–568.
[13] S.A. Mousavi Shaegh, N.-T. Nguyen, S.M. Mousavi Ehteshami, S.H. Chan, Energy Environ. Sci. 5 (2012) 8225–8228.
[14] F. Yang, K. Cheng, X. Xiao, J. Yin, G. Wang, D. Cao, J. Power Sources 245 (2014) 89–94.
[15] F. Yang, K. Cheng, X. Xue, J. Yin, G. Wang, D. Cao, Electrochim. Acta 107 (2013) 194–199.
[16] J.K. Norskov, T. Bligaard, J. Rossmeisl, C.H. Christensen, Nat. Chem. 1 (2009) 37–46.
[17] J. Zhang, K. Sasaki, E. Sutter, R.R. Adzic, Science 315 (2007) 220–222.
[18] D.M. Anjos, F. Hahn, J.M. Léger, K.B. Kokoh, G. Tremiliosi-Filho, J. Solid State Electrochem. 11 (2007) 1567–1573.
[19] Y. Shao-Horn, W.C. Sheng, S. Chen, P.J. Ferreira, E.F. Holby, D. Morgan, Top. Catal. 46 (2007) 285–305.
[20] Y. Kang, F. Chen, J. Appl. Electrochem. 43 (2013) 667–677.
[21] J.-J. Feng, A.-Q. Li, Z. Lei, A.-J. Wang, ACS Appl. Mater. Interfaces 4 (2012) 2570–2576.
[22] S. Zhang, Y. Shao, G. Yin, Y. Lin, Angew. Chem. 122 (2010) 2257–2260.
[23] M. Conte, A.F. Carley, G. Attard, A.A. Herzing, C.J. Kiely, G.J. Hutchings, J. Catal. 257 (2008) 190–198.
[24] G. Lu, C. Li, G. Shi, Chem. Mater. 19 (2007) 3433–3440.
[25] L. Gu, N. Luo, G.H. Miley, J. Power Sources 173 (2007) 77–85.
[26] J.H. Shim, J. Kim, C. Lee, Y. Lee, Chem. Mater. 23 (2011) 4694–4700.
[27] N. Tian, Z.-Y. Zhou, N.-F. Yu, L.-Y. Wang, S.-G. Sun, J. Am. Chem. Soc. 132 (2010) 7580–7581.
[28] X.H. Xia, J.P. Tu, Y.Q. Zhang, Y.J. Mai, X.L. Wang, C.D. Gu, X.B. Zhao, J. Phys. Chem. C 115 (2011) 22662–22668.
[29] H.-C. Shin, M. Liu, Chem. Mater. 16 (2004) 5460–5464.
[30] P. Shahbazi, A. Kiani, Electrochim. Acta 56 (2011) 9520–9529.
[31] R. Li, H. Mao, J. Zhang, T. Huang, A. Yu, J. Power Sources 241 (2013) 660–667.
[32] B. Yang, S. Wang, S. Tian, L. Liu, Electrochem. Commun. 11 (2009) 1230–1233.
[33] H.-B. Noh, K.-S. Lee, P. Chandra, M.-S. Won, Y.-B. Shim, Electrochim. Acta 61 (2012) 36–43.
[34] P. Parpot, S.G. Pires, A.P. Bettencourt, J. Electroanal. Chem. 566 (2004) 401–408.
[35] F. Yang, K. Cheng, K. Ye, X. Wei, X. Xiao, F. Guo, G. Wang, D. Cao, Electrochim. Acta 115 (2014) 311–316.